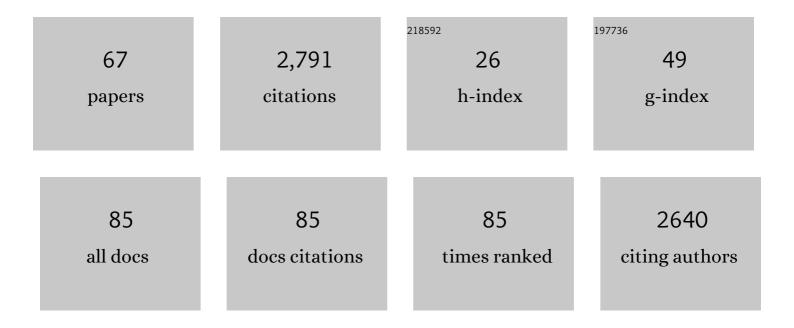
Eric M Pierce

List of Publications by Year in descending order

Source: https://exaly.com/author-pdf/4765844/publications.pdf Version: 2024-02-01



FRIC M DIERCE

#	Article	IF	CITATIONS
1	An international initiative on long-term behavior of high-level nuclear waste glass. Materials Today, 2013, 16, 243-248.	8.3	417
2	Soil Aggregate Microbial Communities: Towards Understanding Microbiome Interactions at Biologically Relevant Scales. Applied and Environmental Microbiology, 2019, 85, .	1.4	233
3	Anaerobic Mercury Methylation and Demethylation by <i>Geobacter bemidjiensis</i> Bem. Environmental Science & Technology, 2016, 50, 4366-4373.	4.6	121
4	In situ remediation technologies for mercury-contaminated soil. Environmental Science and Pollution Research, 2015, 22, 8124-8147.	2.7	102
5	Rapid Removal of Hg(II) from Aqueous Solutions Using Thiol-Functionalized Zn-Doped Biomagnetite Particles. ACS Applied Materials & Interfaces, 2012, 4, 4373-4379.	4.0	96
6	Experimental determination of the effect of the ratio of B/Al on glass dissolution along the nepheline (NaAlSiO4)–malinkoite (NaBSiO4) join. Geochimica Et Cosmochimica Acta, 2010, 74, 2634-2654.	1.6	85
7	Effects of Cellular Sorption on Mercury Bioavailability and Methylmercury Production by <i>Desulfovibrio desulfuricans</i> ND132. Environmental Science & Technology, 2016, 50, 13335-13341.	4.6	78
8	An experimental study of the dissolution rates of simulated aluminoborosilicate waste glasses as a function of pH and temperature under dilute conditions. Applied Geochemistry, 2008, 23, 2559-2573.	1.4	75
9	Contrasting Effects of Dissolved Organic Matter on Mercury Methylation by <i>Geobacter sulfurreducens</i> PCA and <i>Desulfovibrio desulfuricans</i> ND132. Environmental Science & Technology, 2017, 51, 10468-10475.	4.6	74
10	Experimental determination of UO2(cr) dissolution kinetics: Effects of solution saturation state and pH. Journal of Nuclear Materials, 2005, 345, 206-218.	1.3	68
11	Competitive Incorporation of Perrhenate and Nitrate into Sodalite. Environmental Science & Technology, 2014, 48, 12851-12857.	4.6	66
12	Experimentally determined dissolution kinetics of Na-rich borosilicate glass at far from equilibrium conditions: Implications for Transition State Theory. Geochimica Et Cosmochimica Acta, 2008, 72, 2767-2788.	1.6	59
13	Characterization of soils from an industrial complex contaminated with elemental mercury. Environmental Research, 2013, 125, 20-29.	3.7	54
14	Mercury Sorption and Desorption on Organo-Mineral Particulates as a Source for Microbial Methylation. Environmental Science & Technology, 2019, 53, 2426-2433.	4.6	52
15	Accelerated weathering of high-level and plutonium-bearing lanthanide borosilicate waste glasses under hydraulically unsaturated conditions. Applied Geochemistry, 2007, 22, 1841-1859.	1.4	51
16	Understanding the structural drivers governing glass–water interactions in borosilicate based model bioactive glasses. Acta Biomaterialia, 2018, 65, 436-449.	4.1	43
17	Influence of Structural Defects on Biomineralized ZnS Nanoparticle Dissolution: An in-Situ Electron Microscopy Study. Environmental Science & Technology, 2018, 52, 1139-1149.	4.6	42
18	Dissolved organic matter reduces the effectiveness of sorbents for mercury removal. Science of the Total Environment, 2019, 690, 410-416.	3.9	42

ERIC M PIERCE

#	Article	IF	CITATIONS
19	Perrhenate incorporation into binary mixed sodalites: The role of anion size and implications for technetium-99 sequestration. Chemical Geology, 2015, 395, 138-143.	1.4	41
20	Glass–water interaction: Effect of high-valence cations on glass structure and chemical durability. Geochimica Et Cosmochimica Acta, 2016, 181, 54-71.	1.6	36
21	Removal of inorganic mercury by selective extraction and coprecipitation for determination of methylmercury in mercury-contaminated soils by chemical vapor generation inductively coupled plasma mass spectrometry (CVG-ICP-MS). Analytica Chimica Acta, 2018, 1041, 68-77.	2.6	35
22	An insight into the corrosion of alkali aluminoborosilicate glasses in acidic environments. Physical Chemistry Chemical Physics, 2020, 22, 1881-1896.	1.3	35
23	Sequestration and retention of uranium(VI) in the presence of hydroxylapatite under dynamic geochemical conditions. Environmental Chemistry, 2008, 5, 40.	0.7	34
24	Modeling Interfacial Glassâ€Water Reactions: Recent Advances and Current Limitations. International Journal of Applied Glass Science, 2014, 5, 421-435.	1.0	34
25	Mercury Uptake by <i>Desulfovibrio desulfuricans</i> ND132: Passive or Active?. Environmental Science & Technology, 2019, 53, 6264-6272.	4.6	33
26	The Accelerated Weathering of a Radioactive Low-Activity Waste Glass under Hydraulically Unsaturated Conditions: Experimental Results from a Pressurized Unsaturated Flow Test. Nuclear Technology, 2006, 155, 149-165.	0.7	31
27	Modelling the sulfate capacity of simulated radioactive waste borosilicate glasses. Journal of Alloys and Compounds, 2017, 695, 656-667.	2.8	31
28	Experimental determination of the dissolution kinetics of zero-valent iron in the presence of organic complexants. Environmental Chemistry, 2007, 4, 260.	0.7	26
29	Monte Carlo simulations of the corrosion of aluminoborosilicate glasses. Journal of Non-Crystalline Solids, 2013, 378, 273-281.	1.5	26
30	Monte Carlo simulations of the dissolution of borosilicate and aluminoborosilicate glasses in dilute aqueous solutions. Geochimica Et Cosmochimica Acta, 2011, 75, 5296-5309.	1.6	25
31	Aluminoborosilicate waste glass dissolution under alkaline conditions at 40°C: implications for a chemical affinity-based rate equation. Environmental Chemistry, 2008, 5, 73.	0.7	24
32	Deep-UV Raman spectroscopic analysis of structure and dissolution rates of silica-rich sodium borosilicate glasses. Journal of Non-Crystalline Solids, 2011, 357, 2170-2177.	1.5	24
33	Nanomolar Copper Enhances Mercury Methylation by <i>Desulfovibrio desulfuricans</i> ND132. Environmental Science and Technology Letters, 2018, 5, 372-376.	3.9	24
34	Topography and Mechanical Property Mapping of International Simple Glass Surfaces with Atomic Force Microscopy. , 2014, 7, 216-222.		23
35	Immobilization and exchange of perrhenate in sodalite and cancrinite. Microporous and Mesoporous Materials, 2015, 214, 115-120.	2.2	22
36	Quantitative Proteomic Analysis of Biological Processes and Responses of the Bacterium <i>Desulfovibrio desulfuricans</i> ND132 upon Deletion of Its Mercury Methylation Genes. Proteomics, 2018, 18, e1700479.	1.3	22

ERIC M PIERCE

#	Article	IF	CITATIONS
37	Influence of young cement water on the corrosion of the International Simple Glass. Npj Materials Degradation, 2019, 3, .	2.6	22
38	Monte Carlo simulations of the dissolution of borosilicate glasses in near-equilibrium conditions. Journal of Non-Crystalline Solids, 2012, 358, 1324-1332.	1.5	20
39	Experimental determination of the speciation, partitioning, and release of perrhenate as a chemical surrogate for pertechnetate from a sodalite-bearing multiphase ceramic waste form. Applied Geochemistry, 2014, 42, 47-59.	1.4	20
40	Structure and Thermochemistry of Perrhenate Sodalite and Mixed Guest Perrhenate/Pertechnetate Sodalite. Environmental Science & 2017, Technology, 2017, 51, 997-1006.	4.6	19
41	Toward an understanding of surface layer formation, growth, and transformation at the glass–fluid interface. Geochimica Et Cosmochimica Acta, 2018, 229, 65-84.	1.6	19
42	Machine learning–based observation-constrained projections reveal elevated global socioeconomic risks from wildfire. Nature Communications, 2022, 13, 1250.	5.8	19
43	Monte Carlo simulations of coupled diffusion and surface reactions during the aqueous corrosion of borosilicate glasses. Journal of Non-Crystalline Solids, 2015, 408, 142-149.	1.5	18
44	Mercury Adsorption on Minerals and Its Effect on Microbial Methylation. ACS Earth and Space Chemistry, 2019, 3, 1338-1345.	1.2	18
45	Formation of Soluble Mercury Oxide Coatings: Transformation of Elemental Mercury in Soils. Environmental Science & Technology, 2015, 49, 12105-12111.	4.6	17
46	Rates and Dynamics of Mercury Isotope Exchange between Dissolved Elemental Hg(0) and Hg(II) Bound to Organic and Inorganic Ligands. Environmental Science & Technology, 2020, 54, 15534-15545.	4.6	17
47	Isotope exchange between mercuric [Hg(II)] chloride and Hg(II) bound to minerals and thiolate ligands: Implications for enriched isotope tracer studies. Geochimica Et Cosmochimica Acta, 2021, 292, 468-481.	1.6	17
48	Bedrock architecture, soil texture, and hyporheic zone characterization combining electrical resistivity and induced polarization imaging. Journal of Applied Geophysics, 2021, 188, 104306.	0.9	17
49	Mercury-Pollution Induction of Intracellular Lipid Accumulation and Lysosomal Compartment Amplification in the Benthic Foraminifer Ammonia parkinsoniana. PLoS ONE, 2016, 11, e0162401.	1.1	17
50	Efficacy of soluble sodium tripolyphosphate amendments for the in-situ immobilisation of uranium. Environmental Chemistry, 2007, 4, 293.	0.7	15
51	Mineral assemblage transformation of a metakaolin-based waste form after geopolymer encapsulation. Journal of Nuclear Materials, 2016, 473, 320-332.	1.3	13
52	From legacy contamination to watershed systems science: a review of scientific insights and technologies developed through DOE-supported research in water and energy security. Environmental Research Letters, 2022, 17, 043004.	2.2	12
53	Evidence of technetium and iodine release from a sodalite-bearing ceramic waste form. Applied Geochemistry, 2016, 66, 210-218.	1.4	11
54	Performance of the Fluidized Bed Steam Reforming product under hydraulically unsaturated conditions. Journal of Environmental Radioactivity, 2014, 131, 119-128.	0.9	10

ERIC M PIERCE

#	ARTICLE	IF	CITATIONS
55	Combined Experimental and Computational Approach to Predict the Glass-Water Reaction. Nuclear Technology, 2011, 176, 22-39.	0.7	9
56	Energetics of Salt-Bearing Sodalites, Na ₈ Al ₆ Si ₆ O ₂₄ X ₂ (X = SO ₄ ,) Tj ET	ŪqQ 0 0 I	gB∏ /Overloc
	Earth and Space Chemistry, 2020, 4, 2153-2161.	1,2	,
57	Low temperature heat capacity and thermodynamic functions of anion bearing sodalites Na8Al6Si6O24X2 (X = SO4, ReO4, Cl, I). Journal of Chemical Thermodynamics, 2017, 114, 14-24.	1.0	8
58	Characterization of iron oxide nanoparticle films at the air–water interface in Arctic tundra waters. Science of the Total Environment, 2018, 633, 1460-1468.	3.9	8
59	Unravelling biogeochemical drivers of methylmercury production in an Arctic fen soil and a bog soil. Environmental Pollution, 2022, 299, 118878.	3.7	8
60	Dissolution kinetics of a sodium borosilicate glass in Tris buffer solutions: impact of Tris concentration and acid (HCl/HNO ₃) identity. Physical Chemistry Chemical Physics, 2021, 23, 16165-16179.	1.3	7
61	Diffusive release of uranium from contaminated sediments into capillary fringe pore water. Journal of Contaminant Hydrology, 2012, 140-141, 164-172.	1.6	4
62	Development of long-term behavior models for radioactive waste forms. , 2011, , 433-454.		3
63	Mercury source zone identification using soil vapor sampling and analysis. Frontiers of Environmental Science and Engineering, 2015, 9, 596-604.	3.3	2
64	Response to Comment on "Anaerobic Mercury Methylation and Demethylation by Geobacter Bemidjiensis Bem― Environmental Science & Technology, 2016, 50, 9800-9801.	4.6	2
65	Improved ZnS nanoparticle properties through sequential NanoFermentation. Applied Microbiology and Biotechnology, 2018, 102, 8329-8339.	1.7	2

66Competitive exchange between divalent metal ions [Cu(II), Zn(II), Ca(II)] and Hg(II) bound to thiols and
natural organic matter. Journal of Hazardous Materials, 2022, 424, 127388.6.5267Spectroscopic and computational investigations of organometallic complexation of group 12
transition metals by methanobactins from Methylocystis sp. SB2. Journal of Inorganic Biochemistry,
2021, 223, 111496.1.52

5